Available online at www.sciencedirect.com
ScienceDirect
Ceramics International 38 (2012) 713–719
CERAMICS INTERNATIONAL
www.elsevier.com/locate/ceramint

Effect of forming process on the integrity of pore-gradient Al_2O_3 ceramic foams by gelcasting

Xinshuang Guo [a], Zhufa Zhou [a,b,*], Guilin Ma [a], Shumei Wang [a,b], Song Zhao [a], Qiang Zhang [a]

[a] College of Chemistry, Chemical Engineering and Materials Science, Soochow University, Suzhou 215123, PR China
[b] National Engineering Laboratory of Modern Silk, Soochow University, Suzhou 215123, PR China

Received 12 April 2011; received in revised form 14 June 2011; accepted 27 July 2011
Available online 4th August 2011

Abstract

Pore-gradient Al_2O_3 foams were produced by gelcasting using the epispastic polystyrene (EPS) sphere template. This approach allows the design of porous ceramics with degree of pore connectivity and height of gradient layers via appropriate selection of the sizes and numbers of spheres. The fabrication processing of open-cell porous ceramics limited by polymeric sponge template, sharp cracks at the strut edges and closed pores can be resolved by this approach. To achieve the optimal manufacturing conditions of maintaining integrity of the network, the effects of solid loads, height of the slurry and the pre-removal of the polymeric foam template on the struts of the ceramic foams were studied. The results revealed that 55 vol.% Al_2O_3 slurries with 0.5 wt.% ammonium polyacrylate kept good fluidity for casting and avoided the inner inordinate shrinkage. Different shrinkage behavior of the top and bottom of the sample was effectively reduced due to approximately same water vapor diffusion areas on the top and bottom. The integrity of dendritic solidification structure maintained perfectly through template pre-removed in dichloromethane compared with direct heating.
Crown Copyright © 2011 Published by Elsevier Ltd and Techna Group S.r.l. All rights reserved.

Keywords: Integrity; Pore-gradient; Al_2O_3 ceramic foam; Pre-removal

1. Introduction

Gradient porous structure (GPS) means that the size of the pore is not uniform from certain orientation. The pore-gradient continuously changing in diameter or laminate shows the perfect properties of lower filtration resistance, higher separation efficiency, compared with the more general application of ceramic foams. Materials with GPSs can be used as biocompatible implant materials, aerospace, thermal barrier materials and energy conversion applications. Many processing techniques are available to produce porous ceramics and they may be classified into three types: replica methods, sacrificial template, and direct foaming techniques [1,2]. GPS in ceramics had been synthesized by centrifugal molding technique [3], precipitation process [4], replication processing [5], freeze casting [6] or by powder injection molding [7]. The above known techniques are limited to fabricate interconnected GPSs. Many macroporous ceramic structures can be fabricated through the replica technique [8]. Reticulated porous ceramics (RPCs) are typically produced by replicating the connected struts of a polymer template with ceramic slurry. However, their applications are limited by polymeric sponge template, sharp corners at the strut edges [9], closed pores and collapse in sintering, relatively low strength and longitudinal strut cracks [6]. Polymeric sponge sphere is available and cheap and it can constitute all sorts of templates. The internal pores of the template are filled in with ceramic material instead of impregnation of polymeric sponge with slurries, which can avoid the sharp corners at the strut edges and closed pores of RPCs.

Both the macrostructure (i.e. the arrangement of cells) and the microstructure (for instance, the presence of cracks within the struts), have a great influence on the mechanical behavior of the ceramic foams [10]. Thus it is necessary to improve the integrity of processing-related structure of these materials in order to suggest ways of improving both macro and micro-structural designs.

* Corresponding author at: College of Chemistry, Chemical Engineering and Materials Science, Soochow University, Suzhou 215123, PR China. Tel.: +86 0512 65880963; fax: +86 0512 65880089.
E-mail address: zhouzhufa@suda.edu.cn (Z. Zhou).

0272-8842/$36.00. Crown Copyright © 2011 Published by Elsevier Ltd and Techna Group S.r.l. All rights reserved.
doi:10.1016/j.ceramint.2011.07.062

Table 1
Raw materials for this experimental system.

Material	Symbol	Function	Suppliers and characteristics of material
Epispastic polystyrene	EPS	Template	Kunshan Bangjie Packaging Materials Co., Ltd., China, density 0.21 g/cm^3
Alumina	Al_2O_3	Casting matrix	Tianjin Ruidaxinhua Abrasives Co., Ltd., China, density 3.96 g/cm^3, D_{50} = 0.35 μm and a specific surface area of 9.5 m^2/g
Acrylamide	AM	Monomer	Shanghai Chemical Reagent Co., Ltd.
N,N′-methylenebis acrylamide	MBAM	Cross-linker	Hongxing Biological and Chemical Factory of Beijing, China
Ammonium polyacrylate	PAA-NH_4	Dispersant	Jiangsu Institute of Ceramics, China
Ammonium persulfate	$(NH_4)_2S_2O_4$	Initiator	Sinopharm Chemical Reagent Co., Ltd.
Tetramethyl ethylenediamine	TEMED	Catalyst	Sinopharm Chemical Reagent Co., Ltd.
Dichloromethane	CH_2Cl_2	Solvent	Sinopharm Chemical Reagent Co., Ltd.

Gelcasting is a novel process for preparation of near-net-shape ceramic components. Gelcasting process can be developed to fabricate porous ceramics by combining with foaming techniques, replica methods, stacking of pre-sintered granules, or even with the addition of a sacrificial phase [11–13].

One serious problem of high porous materials possessing a large number of organic templates is subject to damage during the removal of the organic template by conventional calcination at high temperature [14]. And structure shrinkage or collapse may occur when the inorganic framework is temperature sensitive [15]. Many methods have been investigated for the template removal. The extraction method of organic template includes supercritical fluid extraction [16], solvent extraction [17], microwave digest [18], UV/H_2O_2 process [15], and UV/ozone treatment [19], which can nondestructively remove the organic template. As the properties of ceramic foams are influenced by their structure, relatively poor mechanical properties are achieved owing to the processing-related flaws [10].

In this study, a novel and feasible method was investigated to fabricate integrative GPS by combining gelcasting process with the epispastic polystyrene (EPS) spheres. By controlling the variation of the sphere size and number distribution, a spatially varied and controllable gradient structure can be created. The struts fabricated by the gelcasting technique are dense and strong, retaining the consolidation of matrix without damage from rebound of packed spheres and reducing the shortcomings of the RPCs mentioned above. This study was to investigate the influence of slurry height on the top of sample and pre-removal of template on the integrity of the pore-gradient Al_2O_3 ceramics. Two methods of pre-removal based on the physical and chemical properties of EPS were grasped.

2. Experimental procedures

Raw materials for this experimental system are listed in Table 1. Fig. 1 shows a flow chart for the overall process of the fabrication of gradient porous Al_2O_3 ceramics. EPS gradient template adopted the arrangement of different sphere sizes and shaped in a bilayer-by-bilayer manner to a required height. Sphere diameters of 1.8 mm, 2.7 mm and 3.2 mm were adopted. Then, the applied force was put to obtain uniform compaction, the whole mold was heated to 130 °C for 10 min to improve the linking strength between the spheres and preserve their deformation. Premix solutions were composed of AM and MBAM with the weight ratio of 20:1. Slurries of different solid contents were prepared by α-Al_2O_3 powder. 0.5 wt.% PAA-NH_4 was added as dispersant in slurries. HCl and NaOH were applied to adjust the pH value. Homogenization was carried out by ball milling for 8 h to adjust the suspension to a proper flowability for casting. Air bubbles were removed in a vacuum desiccator. Gelation began with the addition of $(NH_4)_2S_2O_4$ (0.5 wt.%, based on the weight of AM) and polymerization speed was under the control of TEMED (2 wt.%, based on the weight of AM).

As-prepared Al_2O_3 suspensions were poured into a glass mold (30 mm × 20 mm × 40 mm). A schematic illustration of the instruments for controlling the height was given in Fig. 2. The height of casting slurry was controlled by adjusting floating speeds of slurries. The distance from the center of burette to the

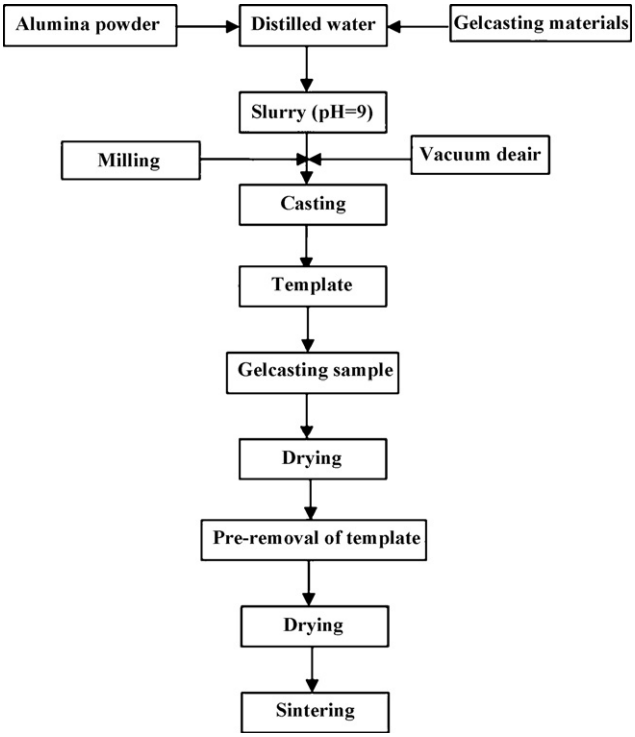

Fig. 1. Flow chart of fabrication of gradient porous Al_3O_2 ceramics using the EPS template.

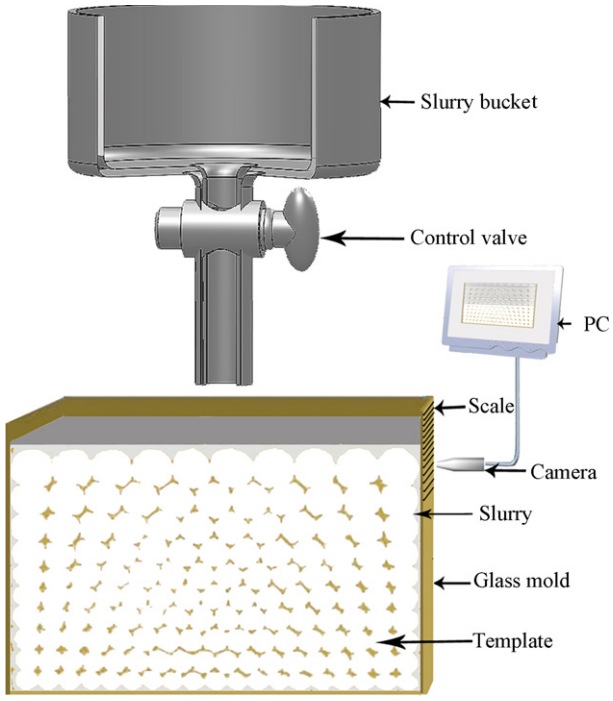

Fig. 2. A schematic illustration of the instruments for controlling the height of slurry.

top of the EPS template was about 10 mm, which provided an appropriate distance to reduce the slurry spilling out and increase measurement accuracy. After slurry up to the desired height for a prescribed time, the sample was taken out from the mold after drying.

The glass transition temperature of the polystyrene polymer is at approximately 108 °C [20]. After heating to this temperature, EPS spheres drastically shrank and became smaller particles, which mostly departed from the substrate after shaking. When treated in dichloromethane, EPS spheres were dissolved and disappeared immediately. In this paper, the templates were pre-removed by heating to 150 °C hold for 2 h and dissolving in dichloromethane, respectively. Water-soluble polyacrylamide (PAM) obtained by the polymerization of AM is nearly insoluble in organic solvents. The solubility and expanded conformation of PAM in solvent were used to estimate the swelling property of a PAM hydrogel.

To study the influence of dichloromethane on the property of PAM and gelcasting struts, they were treated in dichloromethane holding for 10 h and examined by mass or volume change. Viscosity of suspensions was measured with a rotational viscometer (NXS-11A). The length of specimen was measured using micrometer to a precision of ±1 μm. Shrinkage ratio (S_R) was calculated as follows:

$$S_R = \frac{L_T - L_0}{L_0 - L_B} \tag{1}$$

where L_0 is the inner length of mold, L_T the top length of the dried specimen, and L_B the bottom length of the dried specimen. The final value was an average of at least four samples. Stereomicroscope (OLYMPUSSZ61-60) was used to inspect the integrality of networks after the pre-removal of EPS template. Compressive strength of the treated and untreated close gelcasting samples (3 mm × 4 mm × 35 mm) was measured using a universal testing machine (Model 4302, Instron Corp., Canton, MA, USA) with a constant loading rate of 0.5 mm/min and a load cell of 1 kN.

3. Results and discussion

3.1. Effect of solid content on viscosity of suspension

Solid loading has complex influences on the integrity of porous Al_2O_3 ceramics. The reasons are shown as follows.

The influence of viscosity on the permeability coefficient (K_d) can be shown in equation:

$$K_d = \frac{\rho g k}{\eta} \tag{2}$$

where k is the permeability and g is the gravitational acceleration; ρ and η are the density and viscosity of slurry, respectively. According to Eq. (2), the K_d decreases with the increase of η at a given k. As the ceramic slurries become viscous and adhesive by gelation, the internal force from viscosity increases and resists the external force induced by the flow. Thus permeability could hardly occur through the interstitial spaces among the close packed spheres. It can cause pores in the samples and rupture of the struts. The pores in the green specimen would decrease the strength of the green and sintered sample. Therefore, it is necessary to keep the viscosity within a suitable range.

Solid loading has a great influence on the viscosity of Al_2O_3 slurry based on the Woodcock formula [21]:

$$\frac{h}{d} = \left(\frac{1}{3\pi\varphi} + \frac{5}{6}\right)^{1/2} - 1 \tag{3}$$

where h is the space between Al_2O_3 particles in slurry; d the diameter of Al_2O_3 particles and φ the solid loading. From Eq. (3), it is known that the space among Al_2O_3 particles in slurry decreases with the increase of the solid loading, which leads to an increase of the viscosity of the slurry due to the release of immobile liquid within agglomerates. The correlation of solid contents with viscosity of the slurries at 0.5 wt.% dispersant and 150 s^{-1} shear rate is shown in Fig. 3. It can be seen that viscosity of slurries enhanced with the increase of solid content and sharply increases from 55 vol.% to 60 vol.%.

In order to study the effect of solid content on the integrity of sintered strut, assuming that the pore size of the body can be approximated by the hydraulic radius (r_h),

$$r_h = \frac{2(1-\varphi)}{\varphi \rho_s S} \tag{4}$$

where ρ_s is the theoretical density of the slurry and S the specific surface area of particles. It is known from Eq. (4) that the r_h among Al_2O_3 particles in slurry decreases with increasing the solid loading. The transport of liquid through a porous medium is governed by the pressure gradient resulting from capillary pressure [22]. According to Laplace's equation, migration velocity of water vapor is correspondingly enhanced

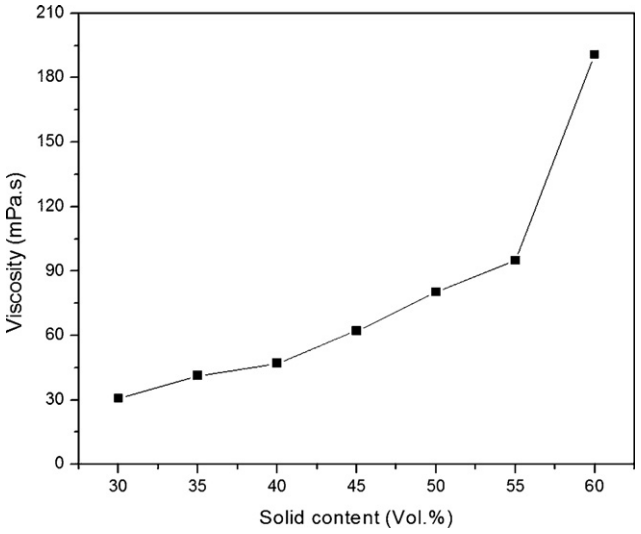

Fig. 3. Viscosity vs. content of dispersant plots of gelcasting slurries with various solid contents.

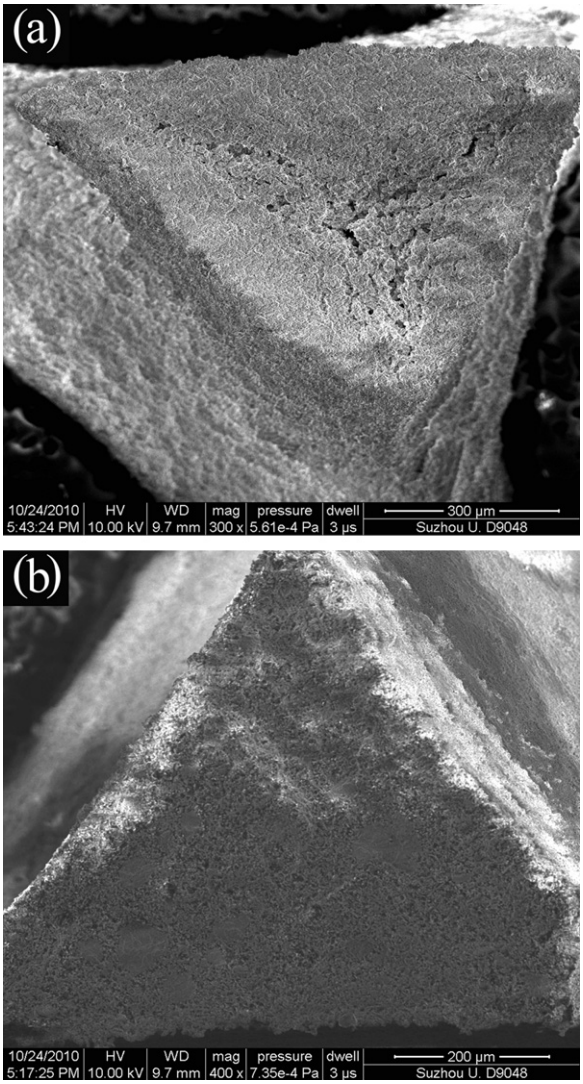

Fig. 4. Microstructures of cross section of the gelcasting sample of different solid contents after sintering at 1500 °C: (a) 30 vol.% and (b) 55 vol.%.

by the capillary pressure. Fig. 4(a) shows microstructural nonuniformities of 30 vol.% Al_2O_3 strut after sintering. Capillary-driven migration of Al_2O_3 particles is expected to occur during drying and sintering, because its size is significantly smaller than the characteristic pore size of the particle network. As φ increases, particle migration is likely suppressed by increasing interactions with neighboring particles. Fig. 4(b) shows dense and crack-free struts of 55 vol.% Al_2O_3 ceramic foams. In order to obtain high permeability coefficient and reduce shrinkage in sintering, slurry with 55 vol.% solid content maintaining good fluidity is employed in this paper.

3.2. Effect of slurry height on shrinkage of the top and the bottom

In order to study the influence of the slurry height on the top and bottom shrinkage ratio of the ceramic body, five different slurry heights were chosen. When the slurry height is 0.5*D* (*D* means the diameter of the top spheres, *D* = 3.2 mm) higher than the highest point of the top spheres, that is the height of the template, the value was defined as 0.5*D*. Similarly the other four

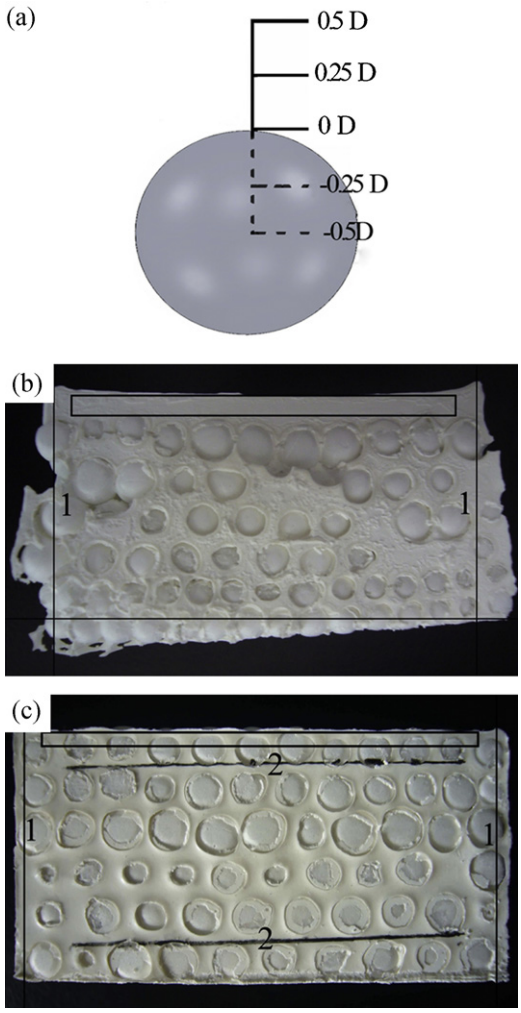

Fig. 5. Pictures of slurry height on the top and bottom of samples after drying: (a) the sketch map, (b) the slurry height at the 0.5*D*, and (c) the slurry height at the −0.25*D*.

Table 2
Statistical evaluation of sample dimension before and after drying in the horizontal and vertical directions.

No	$-0.5D$	$-0.25D$	$0D$	$0.25D$	$0.5D$
Length of the original top and bottom before drying (mm)	30.000	30.000	30.000	30.000	30.000
Length of the top after drying (mm)	29.680	30.023	30.195	31.169	32.641
Length of the bottom after drying (mm)	29.467	29.532	29.624	29.571	29.498
The original height before drying (mm)	15.352	15.358	15.361	15.353	15.356
Height after drying (mm)	16.657	15.964	15.382	15.371	15.375
S_R	−0.600	0.049	0.519	2.725	5.261

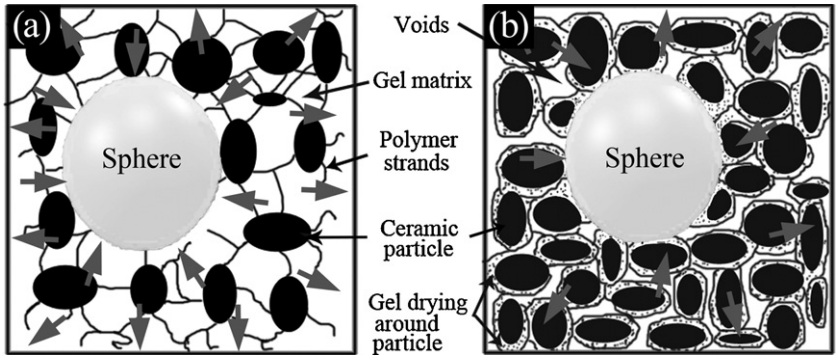

Fig. 6. Sketch map of drying of ceramic foam by gelcasting.

values were named $0.25D$, $0D$, $-0.25D$, $-0.5D$, as it is shown in Fig. 5(a).

Fig. 5(b) ($0.5D$) and Fig. 5(c) ($-0.25D$) shows the effect of top gelcasting slurry height of template on the top and bottom shrinkage ratio of ceramic body dried at 50 °C hold for 18 h. The slurry height on the top of sample was marked with the black rectangle. Vertical line 1 and horizontal line 2 drawn after unmolding are as reference line to show the shrinkage of the top and the bottom in horizontal and vertical direction. The different shrinkage of the top and the bottom can be clearly seen in Fig. 5(b), which leads to the rupture of sample. It can be seen in Table 2 that shrinkage at the $0.5D$ is much larger than that at the $-0.25D$.

When the height of top slurry was $-0.5D$, the shrinkage ratio was −0.6 and the top slurries were separated into isolated parts by spheres in the horizontal direction. Thicker samples correspond to longer transport distances and, hence, their drying rates are much smaller than that of thin gelcasting parts [23]. Transference distance of inner water of the top slurry is shorter than that of the bottom. The tension occurring in the liquid phase induced a corresponding compression of the solid network during drying [24]. So different tension from the top and the bottom of samples causes the minus shrinkage ratio in drying. As shown in Table 2, the coverage area of top template increased with the increase of slurry, discrepancy of shrinkage behavior of the top and the bottom of the specimens increased swiftly.

The drying mechanism is simply shown in Fig. 6. The direction of the arrow indicates diffusion direction of water vapor. Fig. 6(a) shows the Al_2O_3 ceramic particles with little physical contact are uniformly distributed throughout the polymer gel and EPS sphere. In Fig. 6(b) the particles move toward each other and are firmly attached to the polymer network and EPS sphere, when the liquid water is partly transported primarily via capillary forces to the surface after drying. As the whole top template covered by slurry, the effective diffusion area of water vapor decreased from the area of mold and spheres to the area of mold. Thus this diffusion process in gelcasting body is much slower than that in porous gelcasting part. Sample dimension before and after drying in the horizontal and vertical directions is shown in Table 2. It can be seen that the material attempts to relax by expanding in the vertical direction and shrinking in the horizontal direction. The slight elastic relaxation in the vertical direction is easily accommodated since there is no constraint, while the contraction in the horizontal direction is opposed by the constraint that the material base is fixed [25]. It is the stress (tensile stress) that can result in warping and a significantly different shrinkage ratio of the top and the bottom of the specimens. To decrease the shrinkage, water vapor diffusion area of the top and the bottom should be approximate.

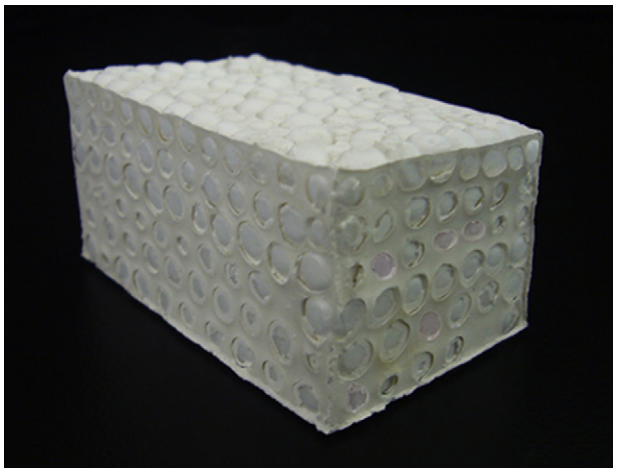

Fig. 7. Shape of sample after unmolding.

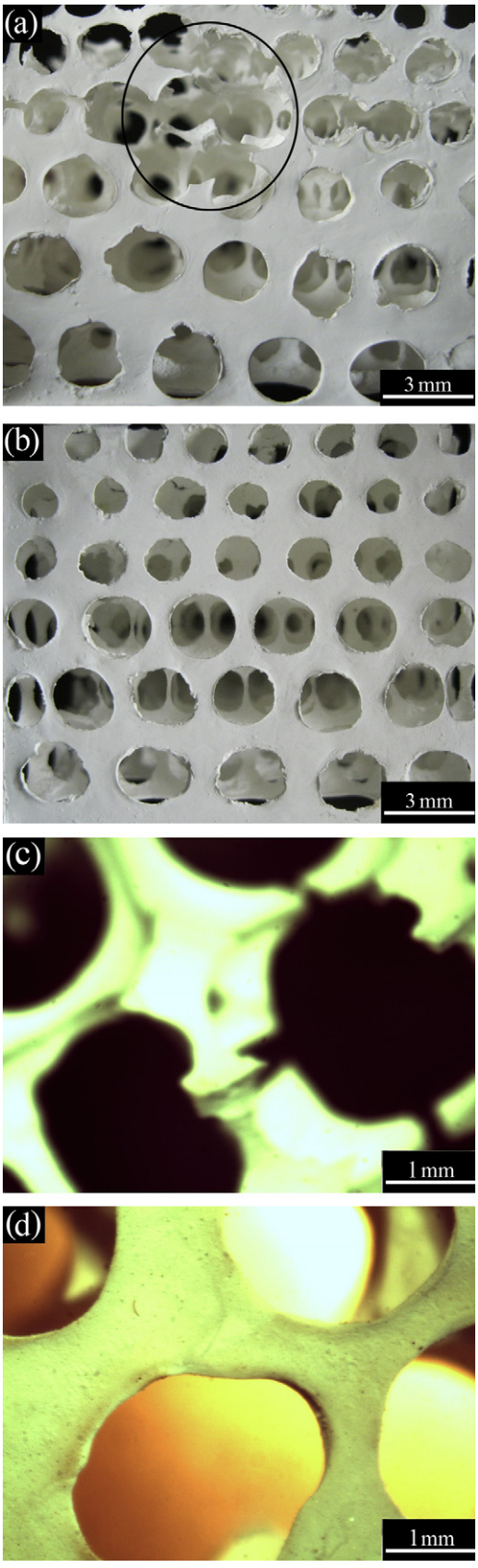

Fig. 8. Macrostructure of porous Al_2O_3 foams obtained by the pre-removal of EPS spheres at different magnification: (a and c) treated in heating; (b and d) treated in dichloromethane.

3.3. Effect of pre-removal of EPS template on integrity of sample

The mass and volume of the PAM do not change after immersed in dichloromethane. The statistical average and standard deviations for compressive strength values were acquired for a total of 5 tests for the treated and untreated gelcasting samples. Their compressive strength average values is approximately taken as 32.7 ± 1.22 MPa. So it was concluded that degradation and solubility of the PAM hydrogel and the destruction of microstructure of gelcasting ceramics do not happen in dichloromethane.

It can be seen that the sample is strong enough to hold the shape after unmolding in Fig. 7. Fig. 8 shows the optical and stereomicroscope pictures of pore-gradient Al_2O_3 ceramic foams through templates pre-removed by heating and dichloromethane after sintering. In Fig. 8(a) the rupture and flaws of the network treated by heating were marked by circle, but in contrast Fig. 8(b) shows that the inner structures and outer surfaces of the pore-gradient samples treated by dichloromethane are flawless ligaments and nearly spherical-shaped walls. Network treated by dichloromethane in Fig. 8(d) remains untouched and contains fewer cracks than that of heating in Fig. 8(c). Polystyrene (PS) has an exceptional ability to bond itself and many common adhesives, such performance makes PS an attractive additive to otherwise difficult-to-bond systems [26]. Closely ordered spheres bond together by adhesive force and shrink to solid particle after release of inner air above glass transition temperature. The smaller particle try to pass windows by tension from adhesive force, which will cause strain to struts of sample. The amount of ligaments gradually decreases with the increase of the strain, resulting in rupture of solid struts and cracks of reticulation points in Fig. 8(a) and Fig. 8(c). For the treatment in solvent, though polystyrene adhesive sticks on the filamentary after extraction from solvent, they hardly influence GPS. Because close contacts have been destroyed and stress from adhesive hardly happens, making this approach suitable to keep the integrality of networks compared with the other approaches.

4. Conclusions

The intact pore-gradient Al_2O_3 ceramic foams were successfully fabricated by gelcasting with adjustable diameters of EPS spheres as templates. The 55 vol.% Al_2O_3 slurry with 5 wt.% dispersant retained sufficient fluidity and high permeability is suitable for casting. The slurry height should keep in a range of $-0.25D$ to $0D$ to reduce the different shrinkage of the top and bottom of sample. The pre-removal of template in dichloromethane, having no destruction on the properties of PAM, prevented bulk defects such as cracks and maintained the integrity of struts compared with direct heating. The sample treated in dichloromethane leaves large pores connected and intact web-like struts after sintering.

Acknowledgements

This work is supported by the National Natural Science Foundation of China (No. 20771079) and the National

Engineering Laboratory of Modern Silk (NELMS, Project No. SS115801), Soochow University, PR China.

References

[1] C. Bartuli, E. Bemporad, J.M. Tulliani, J. Tirillò, G. Pulci, M. Sebastiani, Mechanical properties of cellular ceramics obtained by gel casting: characterization and modeling, J. Eur. Ceram. Soc. 29 (2009) 2979–2989.

[2] J. Luyten, S. Mullens, J. Cooymans, A. Dewilde, I. Thijs, R. Kemps, Different methods to synthesize ceramic foams, J. Eur. Ceram. Soc. 29 (2009) 829–832.

[3] Y. Kinemuchi, Grading porous ceramics by centrifugal sintering, Acta Mater. 51 (2003) 3225–3231.

[4] M.T. Buscaglia, M. Viviani, Z. Zhao, V. Buscaglia, P. Nanni, Synthesis of $BaTiO_3$ core–shell particles and fabrication of dielectric ceramics with local graded structure, Chem. Mater. 18 (2006) 4002–4010.

[5] A. Pollien, Y. Conde, L. Pambaguian, A. Mortensen, Graded open-cell aluminium foam core sandwich beams, Mater. Sci. Eng. A 404 (2005) 9–18.

[6] T.Y. Yang, H.B. Ji, S.Y. Yoon, B.K. Kim, H.C. Park, Porous mullite composite with controlled pore structure processed using a freeze casting of TBA-based coal fly ash slurries, Resour. Conserv. Recycl. 54 (2010) 816–820.

[7] S.X. Zhang, Z.Y. Ong, T. Li, Q.F. Li, S.F. Pook, Ceramic composite components with gradient porosity by powder injection moulding, Mater. Design 31 (2010) 2897–2903.

[8] J. Yu, X. Sun, Q. Li, X. Li, Preparation of Al_2O_3 and Al_2O_3–ZrO_2 ceramic foams with adjustable cell structure by centrifugal slip casting, Mater. Sci. Eng. A 476 (2008) 274–280.

[9] A.R. Studart, U.T. Gonzenbach, E. Tervoort, L.J. Gauckler, Processing routes to macroporous ceramics: a review, J. Am. Ceram. Soc. 89 (2006) 1771–1789.

[10] F. Oliveira, S. Dias, M. Vaz, J. Fernandes, Behaviour of open-cell cordierite foams under compression, J. Eur. Ceram. Soc. 26 (2006) 179–186.

[11] L. Andersson, L. Bergstrom, Gas-filled microspheres as an expandable sacrificial template for direct casting of complex-shaped macroporous ceramics, J. Eur. Ceram. Soc. 28 (2008) 2815–2821.

[12] M. Kokabi, A. Babaluo, A. Barati, Gelation process in low-toxic gelcasting systems, J. Eur. Ceram. Soc. 26 (2006) 3083–3090.

[13] S. Sanchezsalcedo, J. Werner, M. Valletregi, Hierarchical pore structure of calcium phosphate scaffolds by a combination of gel-casting and multiple tape-casting methods, Acta Biomater. 4 (2008) 913–922.

[14] J. He, X. Yang, D. Evans, X. Duan, New methods to remove organic templates from porous materials, Mater. Chem. Phys. 77 (2003) 270–275.

[15] L. Xiao, J. Li, H. Jin, R. Xu, Removal of organic templates from mesoporous SBA-15 at room temperature using UV/dilute H_2O_2, Micropor. Mesopor. Mater. 96 (2006) 413–418.

[16] R. Van Grieken, G. Calleja, G.D. Stucky, J.A. Melero, R.A. Garca, J. Iglesias, Supercritical fluid extraction of a nonionic surfactant template from SBA-15 materials and consequences on the porous structure, Langmuir 19 (2003) 3966–3973.

[17] A. Marcilla, M. Beltran, A. Gómez-Siurana, I. Martínez, D. Berenguer, Evaluation of the efficiency of solvent extraction for template removal in the synthesis of MCM-41 type materials to be used as tobacco additives for smoke toxicity reduction, Appl. Catal. A: Gen. 378 (2010) 107–113.

[18] B. Tian, X. Liu, C. Yu, F. Gao, Q. Luo, S. Xie, B. Tu, D. Zhao, Microwave assisted template removal of siliceous porous materials, Chem. Commun. (2002) 1186–1187.

[19] T. Murakami, Y. Fukushima, Y. Hirano, Y. Tokuoka, M. Takahashi, N. Kawashima, Modification of PS films by combined treatment of ozone aeration and UV irradiation in aqueous ammonia solution for the introduction of amine and amide groups on their surface, Appl. Surf. Sci. 249 (2005) 425–432.

[20] D. Yao, W. Zhang, J.G. Zhou, Controllable growth of gradient porous structures, Biomacromolecules 10 (2009) 1282–1286.

[21] P. Sollich, F. Lequeux, P. Hbraud, M.E. Cates, Rheology of soft glassy materials, Phys. Rev. Lett. 78 (1997) 2020–2023.

[22] D.R. Uhlmann, Ultrastructure Processing of Advanced Materials, Arizona Universisty Tucson, 1992.

[23] S. Ghosal, A. Emami-Naeini, Y.P. Harn, B.S. Draskovich, J.P. Pollinger, A physical model for the drying of gelcast ceramics, J. Am. Ceram. Soc. 82 (1999) 513–520.

[24] J.J. Guo, J.A. Lewis, Aggregation effects on the compressive flow properties and drying behavior of colloidal silica suspensions, J. Am. Ceram. Soc. 82 (1999) 2345–2358.

[25] Y.T. Puyate, C.J. Lawrence, Models for predicting drying stresses and strains in a film cast on a substrate: an alternative approach, Chem. Eng. Sci. 64 (2009) 1820–1831.

[26] Z. Cherian, R. Lehman, Effects of adhesive type and polystyrene concentration on the shear strength of bonded polystyrene/high-density polyethylene blends, Int. J. Adhes. Adhes. 25 (2005) 502–506.